

# Transport and deposition of cohesive pharmaceutical powders in human airway

Yuan Wang\*, Kaiwei Chu, and Aibing Yu

Laboratory for Simulation and Modelling of Particulate Systems, Monash University, Clayton, VIC 3800, Australia

**Abstract.** Pharmaceutical powders used in inhalation therapy are in the size range of 1-5 microns and are usually cohesive. Understanding the cohesive behaviour of pharmaceutical powders during their transportation in human airway is significant in optimising aerosol drug delivery and targeting. In this study, the transport and deposition of cohesive pharmaceutical powders in a human airway model is simulated by a well-established numerical model which combines computational fluid dynamics (CFD) and discrete element method (DEM). The van der Waals force, as the dominant cohesive force, is simulated and its influence on particle transport and deposition behaviour is discussed. It is observed that even for dilute particle flow, the local particle concentration in the oral to trachea region can be high and particle aggregation happens due to the van der Waals force of attraction. It is concluded that the deposition mechanism for cohesive pharmaceutical powders, on one hand, is dominated by particle inertial impaction, as proven by previous studies; on the other hand, is significantly affected by particle aggregation induced by van der Waals force. To maximum respiratory drug delivery efficiency, efforts should be made to avoid pharmaceutical powder aggregation in human oral-to-trachea airway.

## 1 Introduction

To study the flow of inhaled pharmaceutical powders in human airway is important in estimating the health risk of inhaled toxic pollutant and determining the efficacy of aerosol drugs [1]. Pharmaceutical powders used in inhalation therapy are in the size range of 1-5 microns and are usually cohesive. Understanding the cohesive behaviour of pharmaceutical powders during their transportation in human airway is significant in optimising aerosol drug delivery and targeting.

Numerical simulation is widely used by researchers to study the transport and deposition of particles in human airway [2-4]. Most of the studies are based on the assumption of dilute particle flow and the particle level phenomena are usually neglected. In the real-world drug delivery process, however, a large number of particles are injected within a short time and the local particle concentration can be high; particle aggregation may happen due to the cohesive nature of fine particles. Discrete element method (DEM) allows for a detailed description of the particle aggregation process [5]. CFD-DEM coupling model has gained prominent applications in numbers of industrial systems [6] and drug delivery systems [7]. In coupled CFD-DEM model, the motion of particles is modeled by DEM, under which Newton's second law of motion is applied to each single particle; the fluid flow is described by the local averaged Navier-Stokes equations, which can be solved by CFD. Besides of the capability to account for complex interactions

between particles and particle-fluid, coupling of DEM will also provide new physical insight to the fluid-particle dynamics and particle deposition mechanism in human airways.

In this study, a CFD-DEM model is used to describe the particle transport process in human upper airway. The dominant cohesive force, i.e. van der Waals force, is coupled in and the cohesive behaviour of the particle flow is modelled.

## 2 Numerical Methods

### 2.1 Geometry and Mesh

A representative geometry of the adult mouth-throat region is selected for the CFD-DEM model test. The original geometry was developed by Respiratory and Aerosol Dynamics Research Group of Virginia Commonwealth University and described in works by Xi et al [8]. The symmetric plane with cross-sections at several positions and the computational mesh are shown in figure 1. To reduce computation expense, the geometry is down-scaled while the hydrodynamic similarity with real inhalation condition is kept by keeping the same range of the fluid Reynolds number (Re) and particle Stokes number (Stk). The inner space of the model is discretized into a multi-block structured mesh for numerical simulation. The final mesh contains ~112,000 mesh elements, which is determined by a mesh independence study.

\* Corresponding author: [yuan.wang2@monash.edu](mailto:yuan.wang2@monash.edu)

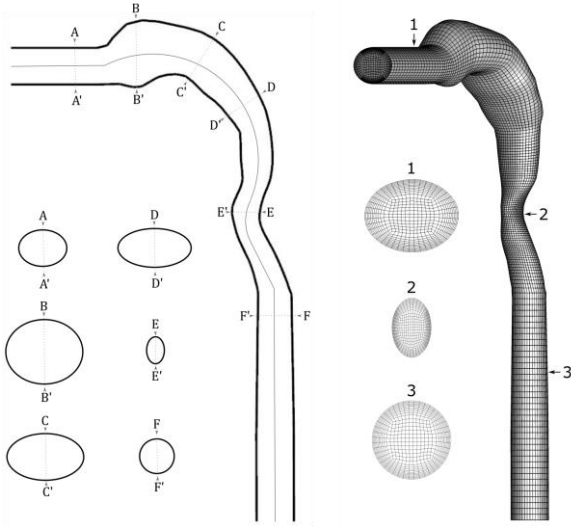


**Fig. 1.** The symmetric plane with cross-sections at several positions and the computational mesh

## 2.2 Governing Equations

The governing equations for the CFD-DEM model have been demonstrated in detail by K. Chu et al [9]. For the continuum phase, the mass and momentum over a computational cell are conserved, leading to the governing equation of fluid flow:

$$\frac{\partial \rho_f \epsilon}{\partial t} + \nabla \cdot (\rho_f \epsilon \mathbf{u}) = 0. \quad (1)$$

$$\frac{\partial (\rho_f \epsilon \mathbf{u})}{\partial t} + \nabla \cdot (\rho_f \epsilon \mathbf{u} \mathbf{u}) = -\nabla P - F_{p-f} + \nabla \cdot (\epsilon \boldsymbol{\tau}) + \rho_f \epsilon \mathbf{g} + \nabla \cdot (-\rho_f \overline{\mathbf{u}' \mathbf{u}'}). \quad (2)$$

where  $\epsilon$ ,  $\bar{\mathbf{u}}$ ,  $\mathbf{u}'$ ,  $t$ ,  $\rho_f$ ,  $P$ ,  $F_{p-f}$ ,  $\boldsymbol{\tau}$  and  $\mathbf{g}$  are, respectively, porosity, mean and fluctuating fluid velocity, time, fluid density, pressure, volumetric fluid-particle interaction force, fluid viscous stress tensor, and acceleration due to gravity.

The particle motion is modelled by discrete element method (DEM) developed by Cundall and Strack [10]. Particle translational and rotational motion is described by Newton's law of motion:

$$m_i \frac{d\mathbf{v}_i}{dt} = \mathbf{f}_{p-f,i} + \sum_{j=1}^{k_i} (\mathbf{f}_{c,ij} + \mathbf{f}_{d,ij} + \mathbf{f}_{vdw,ij}) + m_i \mathbf{g}. \quad (3)$$

$$I_i \frac{d\boldsymbol{\omega}_i}{dt} = \sum_{j=1}^{k_i} (\mathbf{T}_{ij} + \mathbf{M}_{ij}) \quad (4)$$

where  $m_i$ ,  $I_i$ ,  $\mathbf{v}_i$ , and  $\boldsymbol{\omega}_i$  are the mass, moment of inertia, translational velocity and rotational velocities of particle  $i$ , respectively. The inter-particle forces generated by particle collision include the elastic contact force  $\mathbf{f}_{c,ij}$  and viscous damping force  $\mathbf{f}_{d,ij}$ . The cohesive forces arise from van der Waals force ( $\mathbf{f}_{vdw,ij}$ ). Other cohesive forces, e.g., capillary force and electrostatic force are not discussed in current study.

Two-way coupling of CFD-DEM is used in current study, which is achieved by applying Newton's third law in a computational cell. The coupling scheme is well documented in previous literature [11].

## 2.3 Numerical Setup and Boundary Conditions

The numerical solution of the fluid equations (1) and (2) is carried out by commercial finite-volume-based program Fluent 12.0 (Ansys, Inc.). The particle flow is produced by solving equations (3) and (4) by a time integration method. A DEM code is incorporated with Fluent via user defined functions (UDF).

Particles (5 $\mu\text{m}$  in diameter) are injected at mouth inlet with a uniform velocity profile; the air inlet Reynolds number is set to 1000. A uniform pressure boundary condition is applied at the outlets. Other assumptions include incompressible airflow, perfect trapping wall and non-slip wall condition. The physical properties of gas and solid phase are summarized in table 1.

Table 1: Particle and Fluid Properties

Particle Phase	
Particle Diameter ( $\mu\text{m}$ )	5
Particle Density ( $\text{kg/m}^3$ )	1000
Sliding Friction Coefficient	0.3
Damping Coefficient	0.3
Rolling Friction Coefficient	$6 \times 10^{-5}$
Young's Modulus(N/m)	$1 \times 10^{-7}$
Poisson's Ratio	0.3
Hamaker Constant (J)	$6.5 \times 10^{-20}$
Fluid Phase	
Density ( $\text{kg/m}^3$ )	1.225
Viscosity( $\text{kg/m/s}$ )	$1.798 \times 10^{-5}$

## 3 Results and Discussion

The particle transport dynamic is well captured by the CFD-DEM model in current study. To stress the influence of dominant cohesive force, i.e. van der Waals force, the flow patterns of non-cohesive and cohesive particle flow are compared. As illustrated in figure 2, under the influence of van der Waals force, particles start to get aggregated in oral cavity and obvious particle clusters are formed(bottom figure) due to the high local concentration; on the other hand, without cohesive force being coupled in, the particles are still well-dispersed in the same region (top figure).

As particles flowing in the airway, more and more particle clusters are formed and the cluster size becomes larger. Figure 3 describes the particle distribution in the lower part of trachea for non-cohesive and cohesive particle flow. It can be seen that for cohesive particle flow (bottom figure), big clusters are formed and the particle distribution is rather non-uniform at the trachea outlet.

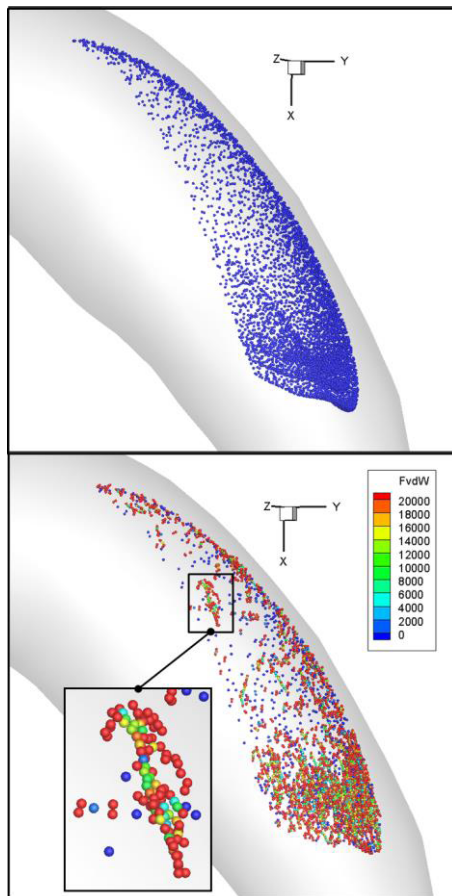


**Fig. 2.** Comparison of particle flow pattern in oral cavity between non-cohesive and cohesive particle flow

In the airway, the wall is assumed to be perfect-trapping wall and thus the clustered particles cannot be deaggregated due to particle-wall impaction. Therefore, the formed clusters can only be deaggregated by fluid drag. In current study, the clusters are assumed to be stable when the particles are bounded by van der Waals force ten times larger than the fluid drag force. Figure 4 illustrates how the mass ratio of the stable clusters to the total particle mass changes with time. It is shown that particle clustered are formed as particles flow in the airway; starting from 0.006s when most of the particles have entered the curved oral cavity, the number of clustered particles are increased more rapidly, which indicates that the curvilinear motion of particles helps the formation of particle aggregation. Later, a steady state is reached where the mass ratio of the clusters no longer changes.

The formation of these particle clusters is predicted to enhance the particle deposition, especially in the subsequent airway bifurcations. As those particle clusters go deeper in the lung, the diameter of each airway is decreasing although their total area is increasing. The ratio of cluster size and airway diameter will get large and the deposition by intersection will become significant.

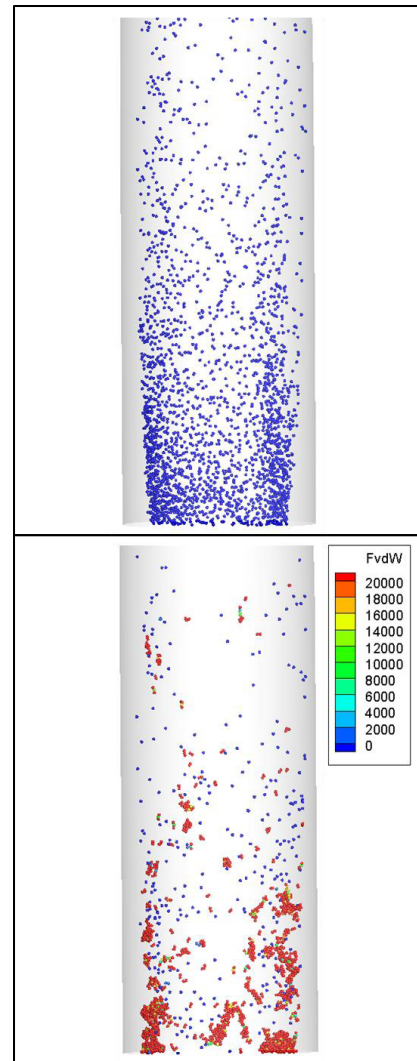


**Fig. 3.** Comparison of particle flow pattern in trachea between non-cohesive and cohesive particle flow

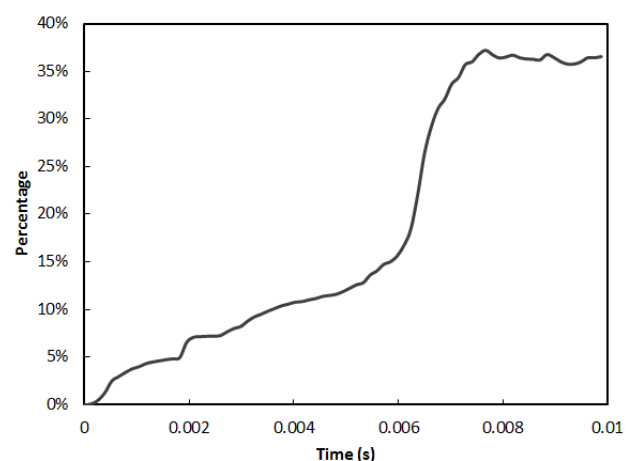


**Fig. 4.** Mass ratio of the stable clusters to the total particle mass plotted with time

## 4 Conclusions

In this study, the transport process of cohesive particle flow is modelled and the influence of van der Waals force is discussed. It is concluded that the cohesive force

leads to significant aggregation in particle flow and the formed particle clusters will enhance particle deposition in human airway. The deposition mechanism for cohesive pharmaceutical powders, on one hand, is dominated by particle inertial impaction, as proven by previous studies; on the other hand, is significantly affected by particle aggregation induced by van der Waals force. To maximum respiratory drug delivery efficiency, efforts should be made to avoid pharmaceutical powder aggregation in human oral-to-trachea airway.

## Acknowledgement

The authors are grateful to the Australia Research Council (ARC) for the financial support.

## References

1. C. A. Ruzycki, E. Javaheri, W. H. Finlay, *Expert Opin. Drug Deliv.* **10**, 3 (2013)
2. B. Soni, S. Aliabadi, *Comput. Fluids* **88**, 0 (2013)
3. M. C. Pigiione, D. Fontana, M. Vanni, *Eur. J. Mech. B-Fluid* **31**, 0 (2012)
4. Y. Feng, C. Kleinstreuer, *J. Aerosol Sci.* **71** (2014)
5. B. H. Xu, A. B. Yu, *Chem. Eng. Sci.* **52**, 16 (1997)
6. S. Limtrakul, A. Boonsrirat, T. Vatanatham, *Chem. Eng. Sci.* **59**, 22–23 (2004)
7. Z. B. Tong, B. Zheng, R. Y. Yang, A. B. Yu, H. K. Chan, *Powder Technol.* **240**, 0 (2013)
8. J. Xi, P. W. Longest, *Ann. Biomed. Eng.* **35**, 4 (2007)
9. K. W. Chu, B. Wang, D. L. Xu, Y. X. Chen, A. B. Yu, *Chem. Eng. Sci.* **66**, 5 (2011)
10. P.A. Cundall, O.D.L. Strack, *Geotechnique* **29** (1979)
11. Z. Y. Zhou, S. B. Kuang, K. W. Chu, A. B. Yu, *J. Fluid Mech.* **661** (2010)